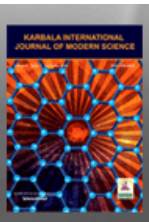
Karbala International Journal of Modern Science

Manuscript 3364

Molecular Docking, Pharmacological Profiling, and Molecular Dynamics Simulation of Potential Antihyperuricemic Agent from Secondary Metabolites of Dillenia philippinensis Rolfe (Dilleniaceae)

Louie Rince C. Suyo

John P. Paulin

Nicole Clarence Louise L. Gapaz

Markus Brent S. Arevalo

Vince Tyrell P. Yongco

See next page for additional authors

Molecular Docking, Pharmacological Profiling, and Molecular Dynamics Simulation of Potential Antihyperuricemic Agent from Secondary Metabolites of Dillenia philippinensis Rolfe (Dilleniaceae)

Abstract

Crystal accumulation in the joints due to increased serum uric acid (sUA) may lead to an inflammatory condition called gout. Increased sUA is caused by the excessive reabsorption of the urate anion transporter-1 (URAT-1). Therefore, URAT-1 inhibition will promote uric acid excretion and reduce the risk of having gout. *Dillenia philippinensis* Rolfe, often known as katmon, is an endemic plant in the Philippines with bioactive compounds associated with several therapeutic benefits. The present study represents the first scientific inquiry into the antihyperuricemic potential of compounds isolated from *D. philippinensis*. This study aimed to assess the interaction of URAT-1 with the bioactive compounds present in katmon through molecular docking and evaluated the pharmacological properties of the compounds. Finally, alanine scanning and molecular dynamics simulation (MDS) were performed with the best-hit compound. The results in molecular docking revealed two compounds with the most stable interaction and high potency. Hence, they were deemed hit compounds. Moreover, pharmacological profiling of these compounds showed that only maslinic acid got accepted remarks based on the Lipinski rule. Additionally, the compound obtained notable results in the Absorption, Distribution, Metabolism, Excretion, and Toxicity (ADMET) assessment. These profiles considered maslinic acid as the best-hit compound. The scanning depicted glutamine 149 as the most significant amino acid in the protein-ligand interaction. Further, relative stable dynamics were obtained in the URAT-1-maslinic acid complex compared to the free protein based on the Root Mean Square Deviation (RMSD) and Root Mean Square Fluctuation (RMSF) values. Our results established the potential antihyperuricemic property of maslinic acid from katmon via URAT-1 inhibition and may exhibit promising pharmacology.

Keywords

Dillenia philippinensis Rolfe, URAT-1, antihyperuricemia, gout, maslinic acid

Authors

Louie Rince C. Suyo, John P. Paulin, Nicole Clarence Louise L. Gapaz, Markus Brent S. Arevalo, Vince Tyrell P. Yongco, and Librado A. Santiago

RESEARCH PAPER

Molecular Docking, Pharmacological Profiling, and Molecular Dynamics Simulation of Potential Antihyperuricemic Agent From Secondary Metabolites of *Dillenia philippinensis* Rolfe (Dilleniaceae)

Louie R.C. Suyo [a,*], John P. Paulin [a], Nicole C.L.L. Gapaz [a], Markus B.S. Arevalo [a], Vince T.P. Yongco [a], Librado A. Santiago [a,b,c]

[a] Department of Biochemistry, Faculty of Pharmacy, University of Santo Tomas, Manila, Philippines
[b] The Graduate School, University of Santo Tomas, Manila, Philippines
[c] The Research Center for Natural and Applied Sciences, University of Santo Tomas, Manila, Philippines

Abstract

Crystal accumulation in the joints due to increased serum uric acid (sUA) may lead to an inflammatory condition called gout. Increased sUA is caused by the excessive reabsorption of the urate anion transporter-1 (URAT-1). Therefore, URAT-1 inhibition will promote uric acid excretion and reduce the risk of having gout. *Dillenia philippinensis* Rolfe, often known as katmon, is an endemic plant in the Philippines with bioactive compounds associated with several therapeutic benefits. The present study represents the first scientific inquiry into the antihyperuricemic potential of compounds isolated from *D. philippinensis*. This study aimed to assess the interaction of URAT-1 with the bioactive compounds present in katmon through molecular docking and evaluated the pharmacological properties of the compounds. Finally, alanine scanning and molecular dynamics simulation (MDS) were performed with the best-hit compound. The results in molecular docking revealed two compounds with the most stable interaction and high potency. Hence, they were deemed hit compounds. Moreover, pharmacological profiling of these compounds showed that only maslinic acid got accepted remarks based on the Lipinski rule. Additionally, the compound obtained notable results in the Absorption, Distribution, Metabolism, Excretion, and Toxicity (ADMET) assessment. These profiles considered maslinic acid as the best-hit compound. The scanning depicted glutamine 149 as the most significant amino acid in the protein-ligand interaction. Further, relative stable dynamics were obtained in the URAT-1-maslinic acid complex compared to the free protein based on the Root Mean Square Deviation (RMSD) and Root Mean Square Fluctuation (RMSF) values. Our results established the potential antihyperuricemic property of maslinic acid from katmon via URAT-1 inhibition and may exhibit promising pharmacology.

Keywords: *Dillenia philippinensis* Rolfe, URAT-1, Antihyperuricemia, Gout, Maslinic acid

1. Introduction

Gout is a condition characterized by inflammation and crystal formation in the joints caused by elevated serum uric acid (sUA) levels in the body [1]. Uric acid (UA) is known to be the final product of purine metabolism [2]. Foods such as red meat, liver, seafood, and beverages like beer contain a significant amount of purines [3]. The urate anion transporter-1 (URAT-1) protein consists of 555 amino acid residues and 12 transmembrane segments, facilitating the UA reabsorption from the lumen to the tubular cells [4]. Reabsorption occurs when UA in the lumen is substituted by organic anions like Cl^-,

Received 18 March 2024; revised 4 July 2024; accepted 7 July 2024.
Available online 1 August 2024

* Corresponding author.
E-mail address: lrcsuyo@gmail.com (L.R.C. Suyo).

https://doi.org/10.33640/2405-609X.3364

Na^+, nicotinate, and pyrazinoate in the epithelial cells [5]. Unlike other transporters that have shown transport activity to various substrates and are multispecific, the transport mechanism of URAT-1 is determined to be specific for UA [6]. Excessive reabsorption of UA may result in increased sUA and can consequently lead to gout [7].

Gout is a prevalent and burdensome condition, with a global prevalence ranging from 1 to 4% and a higher incidence in men and the elderly [8]. Racial and ethnic minorities, indigenous populations, and females are disproportionately affected, with a higher prevalence and incidence of gout [9]. Moreover, the prevalence of gout is exceptionally high in Pacific countries, and some ethnic groups, such as Taiwan's Aborigines, are more susceptible to the condition [10,11]. Current treatments for gout and hyperuricemia come with several drawbacks. Commonly used medications, like non-steroidal anti-inflammatory drugs, colchicine, and corticosteroids, can lead to serious side effects, especially in patients with kidney and heart issues [12]. Additionally, these treatments might not be suitable for everyone, particularly older adults and those with multiple health conditions [12]. The high cost of available uricosuric drugs, such as lesinurad and arhalofenate, also makes them less accessible [13].

Although uricosuric drugs effectively lower uric acid levels, their use comes with significant problems, such as a higher risk of serious kidney concerns [14]. This creates a pressing need for safer treatment options. As a result, attention is turning towards natural compounds that might have inherent URAT-1 inhibitory properties. Exploring these natural alternatives, with their various bioactive components, offers a promising path for creating new and more tolerable gout treatments [15].

Dillenia philippinensis Rolfe (Dilleniaceae), commonly known as katmon, is an endemic plant in the Philippines with antibacterial, antihyperglycemic, and anti-leishmanial effects derived from its secondary metabolites [16–18]. The potential of *D. philippinensis* as a source of antihyperuricemic agents is supported by several studies. Reference [19] discovered that the ethyl acetate fraction of *D. philippinensis* leaf extract has strong xanthine oxidase inhibitory activity, which is crucial for treating hyperuricemia. Moreover, References [20,21] have isolated compounds from *Dillenia indica*, a related species, showing enzyme inhibitory and antidiabetic effects. This suggests that *D. philippinensis* might contain similar beneficial compounds. Additionally, various compounds have been identified in *D. philippinensis*, including a new sulfated glucoside and a new seco-A-ring oleanane-type triterpenoid [16]. Other Dillenia species have also been found to contain potentially therapeutic compounds, such as lupeol and betulinic acids [22]. Over 130 compounds have been identified within the Dilleniaceae family, including flavonoids, terpenoids, lignoids, phenolic derivatives, and other diverse compounds [23]. These findings highlight the chemical diversity in the Dilleniaceae family and their potential for pharmacological exploration.

Furthermore, the functional groups found in well-known uricosuric agents, like 6,7-dichloro-5-sulfamoyl-2,3-dihydrobenzofuran-2-carboxylic acids, are also present in the bioactive compounds identified in various Dillenia species, such as betulinic acid, lupeol, and gallic acid [25,22,24]. The fact that these compounds from Dillenia share similar chemical structures and show bioactive properties provides a solid foundation for considering them effective in treating hyperuricemia. This suggests that Dillenia-derived compounds could become valuable therapeutic options for managing this condition.

To the best of our knowledge, while *D. philippinensis* has been associated with different medical properties, no studies scrutinizing its potential antihyperuricemic properties have been reported. The present study pioneered the in-silico assessments of the interaction between URAT-1 and the bioactive compounds present in *D. philippinensis* through molecular docking experiments, assessed the drug-likeness, pharmacokinetics, and toxicity of the hit compounds through pharmacological analysis, and further validated the docking experiments through alanine scanning mutagenesis and molecular dynamics simulation. This would potentially benefit patients with hyperuricemia and serve as a basis for drug development and the discovery of other beneficial properties of *D. philippinensis*.

2. Materials and methods

This study followed a systematic approach to investigate potential antihyperuricemic agents from *D. philippinensis*. Initially, protein homology modeling was used to predict the 3D structure of URAT-1 based on sequence similarity to known proteins. Ligand preparation involved optimizing the bioactive compounds from *D. philippinensis* for interaction studies. The active site determination identified where these compounds would likely bind to URAT-1. Molecular docking simulated the binding of the ligands to the active site, revealing promising interactions. Pharmacological profiling evaluated the drug-likeness and potential biological effects of the ligands. Alanine scanning mutagenesis assessed the importance of specific amino acids for ligand

binding by substituting them with alanine. Lastly, molecular dynamics simulation provided detailed insights into the stability and behavior of the ligand-protein complex over time, confirming the docking results and predicting the efficacy of compounds in a biological setting. This multifaceted methodology aims to thoroughly assess the therapeutic viability of natural compounds against hyperuricemia and gout.

2.1. Ligand preparation

Reference [23] was utilized to identify the ligands evaluated in this study. Flavonoids, terpenoids, and other chemicals were discovered in *D. philippinensis* (Fig. 1). PubChem was utilized to collect the ligands used in the simulation. The 3D structure of the ligands was then minimized in Avogadro using the auto-optimization parameters and an MMFF94 force field with ten steps per update [26].

2.2. Protein homology modelling

The crystal structure of the glycerol-3-phosphate transporter (PDB ID: 1PW4; resolution: 3.30) was used to predict the structure of URAT-1 [27]. The 1PW4 and URAT-1 protein sequences were aligned in a web-based ClustalW from ExPASy to generate the .pir file and were utilized to predict the URAT-1 structure using MODELLER [28]. The generated structure was minimized through the YASARA

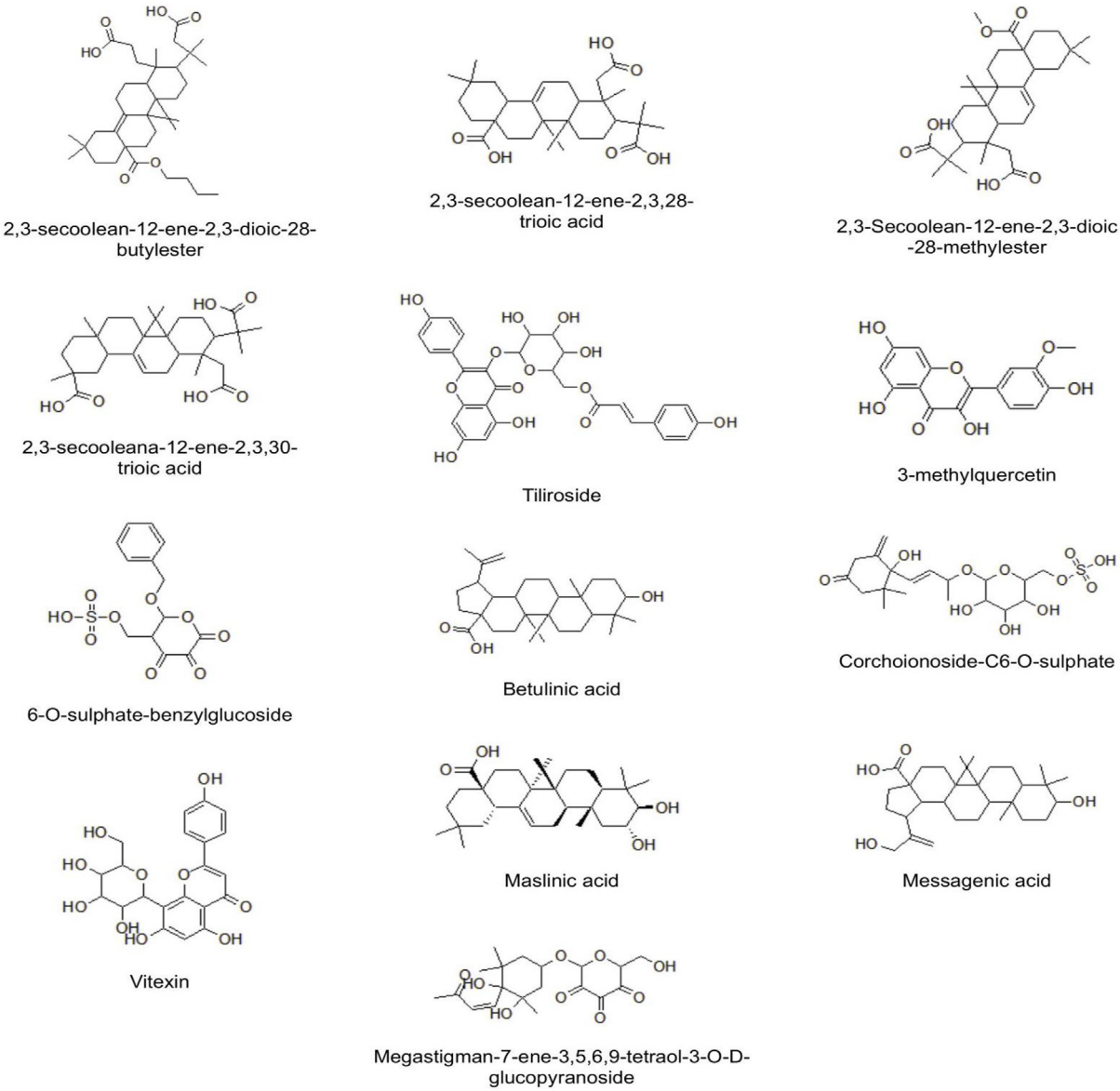

Fig. 1. Structures of compounds from Dillenia philippinensis Rolfe.

force field in the YASARA Energy Minimization server (http://www.yasara.org/minimizationserver.htm) [29]. It was then evaluated using PROCHECK (https://saves.mbi.ucla.edu/) [30], where the Ramachandran plot obtained was used to assess the quality of the constructed protein structure (Fig. 2). Finally, polar hydrogens were added to the 3D structure before docking using BIOVIA Discovery Studio [31].

2.3. Active site determination

The predicted structure of URAT-1 was submitted to CASTp 3.0, and the identified binding pockets were used as the search space for the docking [32]. Uric acid (UA), the URAT-1's substrate, was then blindly docked to the binding pockets identified from CASTp 3.0. The search space values were 32.846 for center x with a size of 60, 21.111 for center y with a size of 66, −35.019 for center z with a size of 76, and an exhaustiveness value of 100.

2.4. Molecular docking

The 3D structures of ligands and URAT-1 were converted to pdbqt format using AutoDockTools. Using the same application, the structure of URAT-1 was identified as the macromolecule for which the data for the search space was obtained using a Grid Box by manually covering a section of the protein where the ligands are expected to bind. The search space values are 33.59 for center x with a size of 20, 13.656 for center y with a size of 20, and −28.859 for center z with a size of 20 and an exhaustiveness value of 100. These specific parameters were loaded into the configuration file used in AutoDockVINA [33]. After docking each ligand, the output files were separated to obtain a distinct record of the poses, including a log file with the collected data of each pose's binding energy in kcal/mol. The split files were inspected and analyzed in BIOVIA Discovery Studio, which revealed the exact amino acids responsible for each pose's binding and the types of

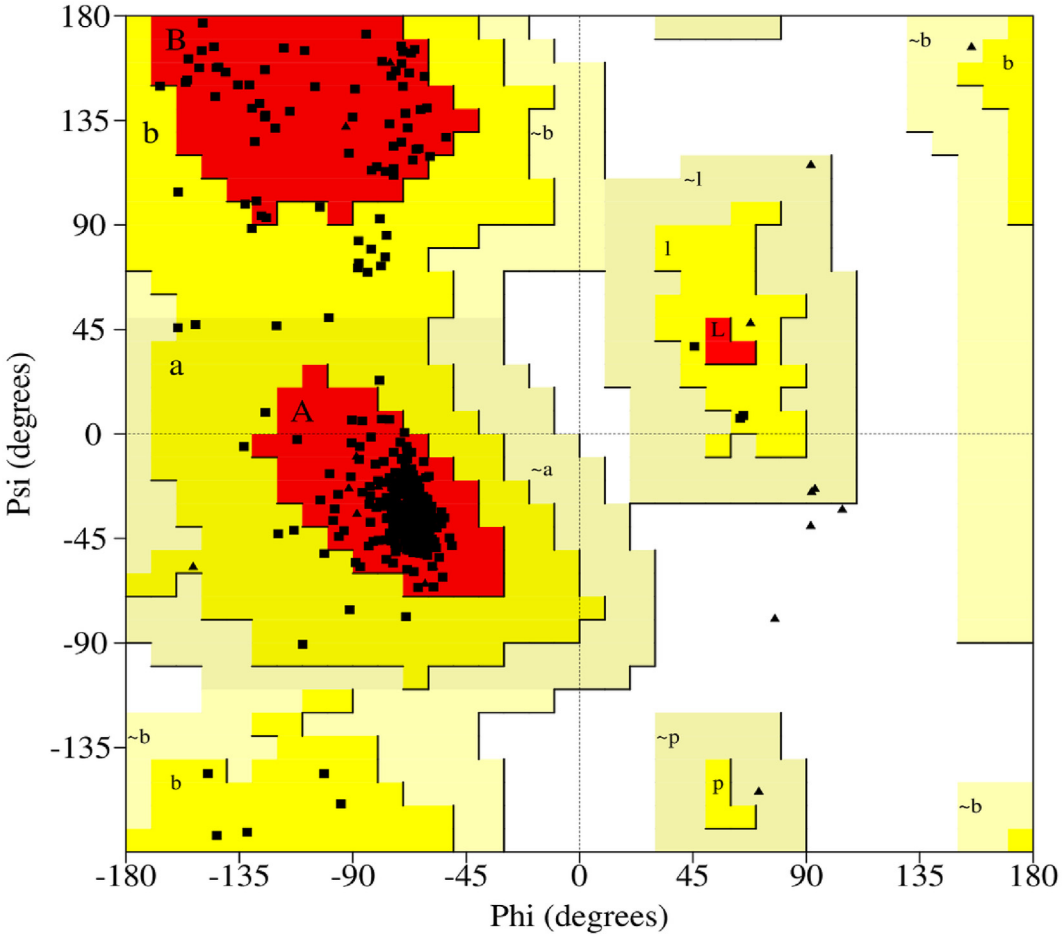

Fig. 2. The Ramachandran plot suggests that the protein has a highly stable conformation, with 89.9% of residues in the most favorable region, 10.1% of residues in the additional allowed region, and 0.0% of residues in the disallowed regions. This is indicative of a well-folded and energetically favorable protein structure.

bonds involved in the ligand-protein interaction. Ligands with similar binding sites to known URAT-1 inhibitors were investigated further in the subsequent analysis. Finally, uric acid was docked again using the parameters mentioned in this section for the verification step. The generated pose was compared with the generated pose of UA from the active site determination step, in which the two structures of UA were superimposed with one another where the RMSD was measured. Finally, the binding affinity scores of the identified hit compounds were used to compute their inhibitory constant (Ki) using the equation below.

$$Ki = e^{\left[\frac{\Delta G}{RT}\right]} \times 10^{6} \mu M$$

where $R = 1.987 \times 10^{-3}$ kcal/K-mol; $T = 298.15$ K

2.5. Pharmacological profiling

Drug-likeness evaluation was performed using molinspiration (https://www.molinspiration.com/) to obtain the properties of the chemical space of the compounds. Such properties include molecular weight (MW), heavy atoms (HA), no. of violations, hydrogen-bond donor (HBD), hydrogen-bond acceptor (HBA), and miLogP, which are the properties being evaluated by the Lipinski rule [34]. This guideline was employed to qualitatively evaluate a molecule's potential as an oral drug in terms of bioavailability. The cLOGP and Lipinski results were obtained from SwissADME (http://www.swissadme.ch/) [34].

Pharmacokinetic profiles of the bioactive compounds were determined using ADMETLab 2.0 (https://admetmesh.scbdd.com/) and SwissADME web servers [35,34]. The canonical SMILES of the molecule or compound are found in the PubChem Database (https://pubchem.ncbi.nlm.nih.gov/) and can be directly pasted or typed in SMILES format on both web servers. In addition, compounds not available in the PubChem Database were drawn in ChemSketch and converted to the corresponding canonical SMILES format. Specifically, Absorption, Distribution, Metabolism, Excretion, and Toxicity (ADMET) parameters that were included in the assessment were human intestinal absorption (HIA) and permeability glycoprotein (P-gp) for absorption; blood–brain barrier (BBB), plasma protein binding (PPB), fraction unbound (FU), and volume distribution (VD) for distribution; cytochrome P450 isoenzymes 1A2, 2C19, 2C9, 2D6, and 3A4 for metabolism; clearance (CL) and half-life (T1/2) for excretion; and lastly, hERG blocker, human hepatotoxicity (HHT), drug-induced liver injury (DILI), and AMES toxicity for toxicity.

2.6. Alanine scanning mutagenesis

Amino acid residues interacting with the best-hit compound were subjected to alanine scanning mutagenesis. The residues identified were substituted with alanine in the sequence one by one. The mutants' structures were produced using the same parameters in protein homology modeling. The best-hit compound was docked with each generated mutant using the same parameters employed in the molecular docking experiment. Finally, the binding energy differences (ΔΔG) were measured and compared with that of the wild-type protein.

2.7. Molecular dynamics simulation

GROMACS was utilized for the molecular dynamics simulation (MDS) of the URAT-1 best-hit compound-complex. The ligand's topology file and parameter files were made using the LigParGen web server, whereas the topology file of URAT-1 was generated using the pdb2gmx command and the OPLS-AA/L all-atom force field. The complex was then solvated in a cubic box using a TIP3P water model and immersed in SPC216 with a setback distance of 1.0 nm between the complex and the box's border. Consequently, the system was neutralized by adding eight chloride ions to the solvent. The system was then minimized and equilibrated for 100 ps under constant NVT and NPT, with a temperature of 300 K and a pressure of 1.01325 bar. Finally, the complex underwent a manufacturing process lasting 10,000 ps, during which the RMSD and RMSF of the protein backbone were measured. The procured results were then evaluated against the results obtained from the MDS of the unbound URAT-1.

3. Results and discussion

3.1. Active site determination

CASTp (Computed Atlas of Surface Topography of proteins) analysis of URAT-1 protein has revealed a binding pocket with a (Richards') solvent-accessible area and volume of 2830.336 Å2 and 2459.861 Å3, respectively (Fig. 3). The location of the identified binding sites was used as the search space for UA's blind docking. Moreover, the blind docking analysis revealed that UA has interacted with residues Asn39, Met36, and Gln149 from transmembrane 1, Ala368 from transmembrane 7, and

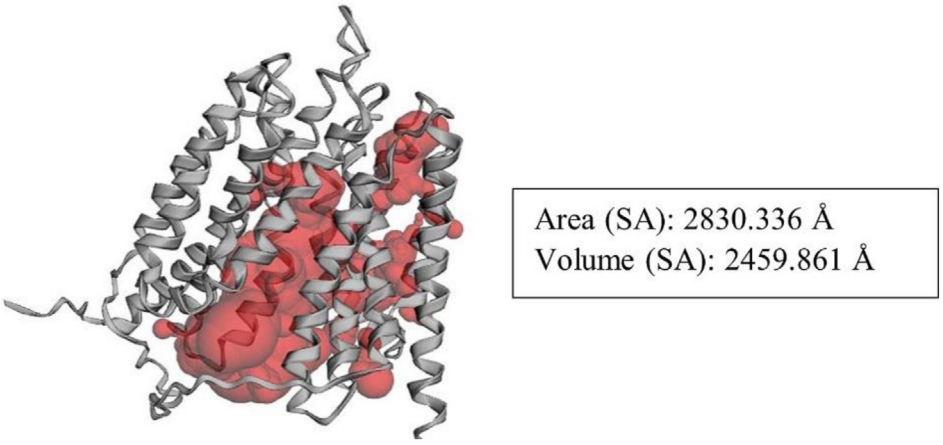

Fig. 3. CASTp analysis of URAT-1. The identified binding pocket served as a guide for further analysis.

Pro484 from transmembrane 11. Additionally, UA demonstrated hydrogen bonding with residues Asn39 and Pro484 and hydrophobic interactions with residues Met36, Gln149, and Ala368, which accounts for a binding affinity of $\Delta G = -6.1$ kcal/mol (Figs. 4 and 5). Reference [36] confirmed that the elucidated active site of UA is accurate, where the transmembranes 1, 7, and 11 were identified to be responsible for the interaction of both the uricosuric drugs and UA. However, the residues identified to interact with UA from the abovementioned study did not match those identified in this study. Nonetheless, the discrepancy between these studies reveals the necessity for further verification as the presence of the residues identified by the abovementioned study may also result in a conformational change with the protein structure, specifically in its binding pocket that is suitable for the binding of uricosuric drugs and UA [37,38]. It should be noted that the study mentioned that the role of substrate transport can be one of the plausible reasons for the conformational changes that occur during the simulation [36]. Both simulations used the bacterial glycerol-3-phosphate transporter as the template of the protein for the docking. Therefore, establishing the URAT-1 crystal structure could help determine the precise position of the residues in the mentioned transmembranes.

3.2. Molecular docking analysis

The result of molecular docking revealed that among the bioactive compounds in *D. philippinensis*, tiliroside and maslinic acid have exhibited two of

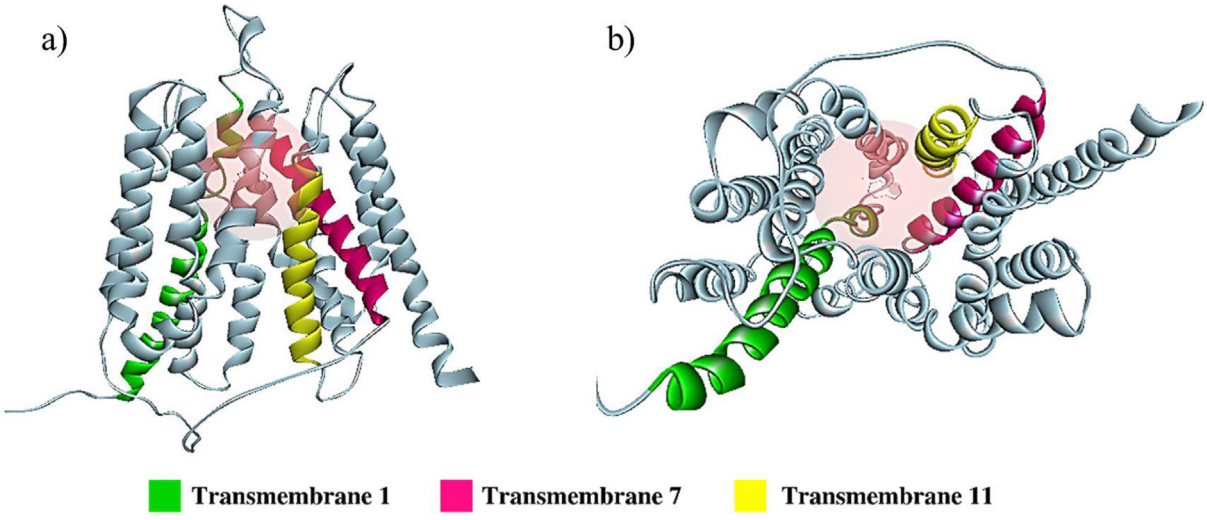

Fig. 4. Active site of URAT-1 determined through blind docking presented in (a) side view and (b) bottom view. Uric acid has interacted with URAT-1 inside a pocket in the middle of TM1, TM7, and TM11 which served as the active site.

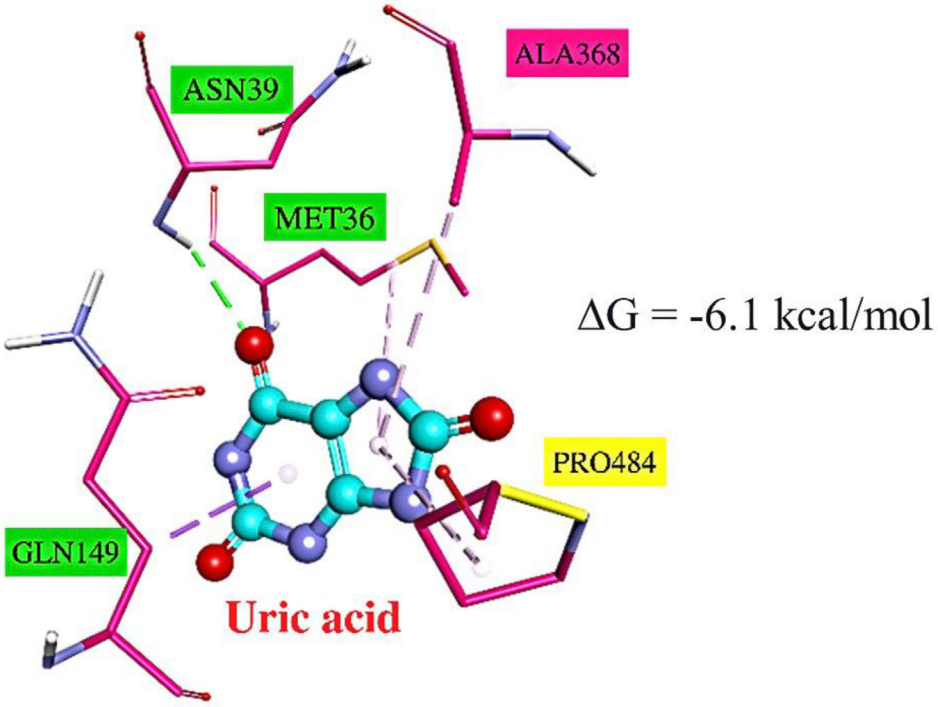

Fig. 5. Molecular interactions between uric acid and URAT-1 at transmembranes 1, 7, and 11. Uric acid exhibited interactions with residues from TM1, 7, and 11 as observed in Fig. 4.

the highest binding affinities with binding energies of −9.4 and −8.6 kcal/mol, respectively. Both compounds formed hydrogen and hydrophobic interactions that are comparable to the binding of known URAT-1 inhibitors losartan, sulfinpyrazone, benzbromarone, lesinurad, and probenecid with binding affinities of −9.0, −8.8, −8.2, −7.1, and −6.9 kcal/mol, respectively. Interestingly, their binding affinities with URAT-1 were relatively higher than its substrate, UA (ΔG −6.1 kcal/mol). Negative binding energies signify a stable compound with receptor molecules, indicating an effective medication [39].

Tiliroside formed hydrogen and hydrophobic interactions comparable to known uricosuric drugs. In particular, hydrogen-binding was formed at Ser35, which was also present in losartan and sulfinpyrazone. Meanwhile, hydrophobic interactions at Tyr152 were observed in benzbromarone and losartan, Leu153 in probenecid and sulfinpyrazone, Phe364 in probenecid, sulfinpyrazone, and lesinurad, Ala476 in losartan, sulfinpyrazone, and lesinurad, and Ala480 in benzbromarone, probenecid, sulfinpyrazone, and lesinurad. Meanwhile, maslinic acid formed hydrogen bonding with only three residues, Gln149, Phe364, and Pro484, where interactions at Phe364 and Pro484 were similar to those involved with known URAT-1 inhibitors. Particularly, interactions at Phe364 were also present in probenecid, lesinurad, and sulfinpyrazone, whereas interaction at Pro484 is also present in benzbromarone, losartan, probenecid, and sulfinpyrazone. Both Gln149 and Pro484 residues participated in the interaction of URAT-1 with its substrate, UA. The findings indicated that hydrogen and hydrophobic interactions at different amino acid residues were important in forming a stable protein-ligand complex. Hydrophobic interactions influence the stability of proteins, while hydrogen bonding contributes to the stability of the protein-ligand complex to a lesser extent [40].

The docked ligands' inhibition constants (Ki) ranged from 0.13 μM to 33.74 μM. Among the 13 ligands, tiliroside and maslinic acid, with Ki values of 0.13 μM and 0.5 μM, respectively, exhibited inhibition constants within the suggested range of 0.1 μM and 1.0 μM. Only ligands with inhibition constants within this range are considered hit compounds, which were then subjected to pharmacological analysis. The lower the Ki value, the higher the potency or inhibitory efficacy, provided that it is within the acceptable range [41].

Uric acid was docked again after the molecular docking analysis of the bioactive compounds using the parameters used in the molecular docking analysis (specific docking). The docking of UA

revealed interactions with URAT-1 residues Asn39 and Pro484, which formed hydrogen-binding interactions, and Met36, Gln149, and Ala368, which formed hydrophobic interactions. Likewise, the interaction of UA with URAT-1 exhibited a binding affinity of $\Delta G = -6.1$ kcal/mol (Table 1). The redocking of UA demonstrated identical interactions with URAT-1 that were observed from the active site determination step (blind docking). This was further analyzed by superimposing the structural poses of UA that were generated from the blind and specific docking, which exhibited an RMSD value of 0.0065 Å.

Ultimately, the purpose of redocking uric acid in the molecular docking analysis is to validate the docking results. By showing that UA interacts with URAT-1 residues consistently and yields a similar binding affinity during both blind docking and specific docking, the study confirms the reliability of the molecular docking process.

The low root mean square deviation value indicates a high level of agreement between the docked poses in both phases, which serves as strong evidence that the molecular docking method employed is accurate and can be trusted for evaluating the interactions between URAT-1 and the compounds from *D. philippinensis.* This redocking allows for predicting the predominant binding modes of a ligand with a protein, aiding in lead optimization [42].

3.3. Pharmacological profiling

Drug-likeness serves as a crucial phase in drug discovery, so the "hit to lead" progression of a drug is initially analyzed [34]. Guidelines to predict the

Table 1. Molecular docking results of the terpenoids, glycosides, flavonoids, URAT-1 inhibitors, and uric acid.

Name of Ligands	Binding Affinity, ΔG (kcal/mol)	Inhibition Constant, Ki (μM)	Hydrogen Bonds Interaction	Hydrophobic Interaction
Terpenoids				
2,3-Secoolean-12-ene-2,3-dioic-28-butyl ester	−7.4	3.76	Ser35, Arg203, Pro484	Leu153, Ile156, Leu157, Phe241, Ala476
2,3-Secoolean-12-ene-2,3-dioic-28-methyl ester	−7.7	2.27	Asn39	–
2,3-Secoolean-12-ene-2,3,28-trioic acid	−7.5	3.18	–	Phe241
2,3-Secoolean-12-ene-2,3,30-trioic acid	−7.5	3.18	Asn39	
Betulinic acid	−7.5	3.18	–	Phe364, Ala368, Ala480, Pro484
Maslinic acid	−8.6	0.50	Gln149, Phe364, Pro484	–
Messagenic acid	−8.1	1.15	–	Tyr152
Glycosides				
6′-O-sulphate benzyl glucoside	−7.2	5.27	Cys32, Ser35, His245	Phe241, Phe364, Val445
Corchoionoside C6′-O-sulphate	−7.7	2.27	Tyr152	–
Megastigman-7-ene-3, 5,6,9- tetraol 3-O-D-glucopyranoside	−8.1	1.15	Gln149	–
Flavonoids				
Tiliroside	−9.4	0.13	Ser35, His245, Thr363	Tyr152, Leu153, Phe241, Phe360, Phe364, Val445, Ala448, Ala476, Ala480
3-methylquercetin	−7.7	2.27	Phe364, Ser35	Met36, Phe241, Ala368, Pro484, Ala480
Vitexin	−6.7	12.26	Tyr152	Arg203, Ala480
URAT-1 inhibitors				
Benzbromarone	−8.2	0.97	–	Tyr152, Ala480, Met36, Ala368, Pro484
Lesinurad	−7.1	6.24	Gln473	Phe364, Phe241, Ala480, Ala476
Losartan	−9.0	0.25	Pro484, Ser35	Ala476, Phe241, Leu206, Arg203, Tyr152
Probenecid	−6.9	8.74	Gln34	Pro484, Ala368, Leu153, Ala480, Phe364, Tyr152
Sulfinpyrazone	−8.8	0.35	Ser35	Leu31, Cys32, Ala476, Ile156, Leu153, Ala480, Met36, Pro484, Phe364
URAT-1 substrate				
Uric Acid	−6.1	33.74	Pro484, Asn39	Met36, Ala368, Gln149

drug-likeness of a compound are possible using Lipinski's Rule of Five [43]. Specifically, the rule predicts that the probability of poor absorption is higher when there are more than five H-bond donors and 10 H-bond acceptors, the calculated logP (ClogP) is greater than five, and the molecular weight is greater than 500 g/mol [43]. As shown in Table 2, tiliroside got a rejected Lipinski score, while both maslinic acid and losartan obtained accepted scores, which entail a high potential to become a drug. Moreover, milogP, referred to as the octanol–water partition coefficient logP computed by molinspiration, is included to provide details about the measure of the hydrophobicity of compounds [44]. In addition to lipophilicity, the hydrophobic nature of a drug significantly influences its absorption in the gastrointestinal tract [45]. The bioavailability of drugs may also be affected by this characteristic of the molecule, which will be further discussed in the succeeding tables. The expected miLogP values of the compounds should be equal or less than five to enhance their drug-like properties [46]. Based on the results, tiliroside got a value within the optimal miLogP range. Maslinic acid, which has a greater than five miLogP values, still obtained an accepted result in the Lipinski assessment plausibly because the score only tackles specific aspects of solubility. Lastly, losartan obtained accepted results as expected because this drug exhibits Lipinski properties within the acceptable ranges.

When a compound is administered, it is absorbed into the systemic circulation, where it is subsequently distributed throughout the body [47]. Several factors influence the pace and degree of medication absorption, including route and mode of administration and the physicochemical properties [48]. As shown in Table 3, among the hit compounds, only maslinic acid obtained high remarks on human intestinal absorption (HIA). Interestingly, when compared to the standard drug, which also got high remarks, maslinic acid has a high potential to become a drug, considering its promising absorption. Since oral medicines have decreased drug

Table 2. Drug-likeness properties of the hit compounds and the standard uricosuric drug.

Compound	Molecular Weight (MW)	Heavy Atoms (HA)	No. of Violations	HBD	HBA	miLogP	ClogP	Lipinski Rule
Maslinic acid	472.71	34	1	3	4	5.81	77.75	Accepted
Tiliroside	594.52	43	3	7	13	2.49	216.58	Rejected
Losartan (standard drug)	422.92	30	0	2	7	4.87	92.52	Accepted

Table 3. ADMET prediction of the hit compounds and the standard uricosuric drug.

Properties		Hit Compounds		Standard Uricosuric Drug
		Maslinic Acid	Tiliroside	Losartan
Absorption	Human Intestinal Absorption (HIA)	excellent	poor	excellent
	P-gp substrate	excellent	medium	excellent
Distribution	BBB permeant	No	No	No
	PPB	98.218%	99.250%	97.446%
	FU	4.389%	2.576%	1.652%
	VD	0.802	0.590	0.829
Metabolism	CYP1A2 inhibitor	no	no	no
	CYP2C19 inhibitor	no	no	yes
	CYP2C9 inhibitor	no	no	yes
	CYP2D6 inhibitor	no	no	yes
	CYP3A4	no	no	yes
Excretion	Clearance (CL)	1.487	4.630	6.597
	$T_{1/2}$	0.023	0.787	0.689
Toxicity	hERG blocker	−−−	−−	−
	Human Hepatotoxicity (HHT)	−−	−−−	++
	Drug-induced liver injury (DILI)	−−−	+++	+++
	AMES Toxicity	−−−	++	−−−

Human Intestinal Absorption (HIA) and permeability glycoprotein (P-gp): excellent, medium, poor; **plasma protein binding (PPB):** ≤ 90%: excellent; otherwise: poor; **volume distribution (VD):** 0.04–20: excellent; otherwise: poor; **Fraction Unbound (FU):** >20%: High; 5–20%: medium; <5% low. The unit of predicted **clearance (CL)** is ml/min/kg. >15 ml/min/kg: high clearance; 5–15 ml/min/kg: moderate clearance; <5 ml/min/kg: low clearance; **half-life ($T_{1/2}$)** 0–0.3: excellent; 0.3–0.7: medium; 0.7–1.0: poor. **hERG blocker, HHT, DILI:** negative(−) and positive(+).

absorption due to the first-pass effect to the site of action, the compounds must exhibit a high remark in this parameter [47]. Therefore, highlighting this parameter is crucial to predict the capacity of a potential compound to penetrate through the intestinal walls and reach its target site. Furthermore, xenobiotics can enter the cell via active transport or passive diffusion and can be effluxed using P-gp [49]. This protein is spread throughout the body and can be found in the small intestine, capillaries of the blood–brain barrier, and other essential organs such as the kidney and liver, allowing it to function as a drug-extracting pump [50,51]. This study included information about the compounds that can be a substrate of P-gp to provide additional information about the bioavailability of the compounds since this protein further limits the penetration of a compound in sensitive tissues. As a substrate, the compound may act as an inducer or inhibitor of the protein. Based on the results, only maslinic acid and losartan are considered as P-gp substrates.

As mentioned, a pharmacokinetic parameter that may provide further details about the efficacy of a particular compound is distribution. This parameter focuses on the rate of drug accumulation in peripheral compartments rather than the extent of the drug accumulation [47]. One of the most crucial distribution parameters is the blood–brain barrier (BBB) permeability [52]. The BBB is the 'barrier' that regulates material, nutrition, and cell transport from the bloodstream to the brain and vice versa [52]. As depicted in Table 3, none of the compounds shows BBB penetrating potential. This is still a good quality because the compounds of interest are not assumed to have neurological targets and effects. Moreover, Reference [53] has mentioned that plasma protein binding (PPB) significantly affects the distribution of the drug from plasma to target tissues where it exhibits its pharmacological effect. Extensive binding to these proteins may attenuate the therapeutic properties of drugs because drugs bound to the proteins would find it difficult to enter tissues [53]. Additionally, volume distribution (VD) and drug clearance (CL) are affected when PPB values are high enough [53]. It is because VD describes the extent to which a substance is distributed from plasma into tissues, and only unbound molecules of a drug, as presented by the fraction unbound (FU), may enter the tissues and be subjected to hepatic clearance [54]. Based on the results, none of the hit compounds got excellent remarks. However, one interesting property that can be observed in maslinic acid is its relatively high FU percentage compared to tiliroside and losartan. Reference [55] highlighted that there are still a lot of factors to consider when relating PPB and drug efficacy. On this note, further analyses are done to determine the following factors: (1) the importance of PPB for a specific medicinal application; (2) the type of proteins involved; (3) the effects of pH and temperature; and lastly (4) the essence and requirement of protein displacement drug interactions [55].

Drug elimination is defined as the process of removing the drugs that are introduced into our bodies [56]. In the scheme of pharmacokinetics, both metabolism and excretion have essential roles in the elimination [56]. Moreover, to be eliminated, hydrophobic drugs must undergo metabolic change to become more polar. In contrast, hydrophilic molecules can be excreted without the need to be subjected to metabolic modifications in their molecular structures [56]. As shown in Table 3, metabolism is mainly attributed to five cytochrome P450 isozymes, namely CYPs 1A2, 2C19, 2C9, 2D6, and 3A4, which metabolize approximately two-thirds of known drugs in humans [57]. Specifically, these CYP450 isozymes carry out oxidation, reduction, hydrolysis, and hydroxylation reactions, which are all part of phase I in drug metabolism with the primary goal of increasing the polarity of compounds, especially the highly lipophilic ones [57]. Based on the results, none of the hit compounds inhibit any CYP isozymes. On the other hand, losartan recorded a possible inefficient metabolism as this drug has the potential to inhibit all the isozymes except CYP 1A2. Several drugs' responsiveness and toxicity are affected by CYP450 enzymes [58]. Molecules that inhibit enzymes essential in drug metabolism tend to produce adverse effects [58]. This is because, in terms of metabolic liability, such inhibition can lead to a variety of issues, such as decreased bioavailability due to increased clearance, toxic side effects from drug buildup, and induction, drug–drug interactions like enzyme inhibition, and mechanism-based inactivation [59–61].

On the other hand, the excretion of the drug can be predicted using the scores in clearance (CL) and T1/2 [62]. Both are influenced by VD and PPB because, in a general sense, hepatic clearance affects solely the unbound drug [63]. Based on the result, both hit compounds and losartan obtained low clearance. However, maslinic acid obtained excellent half-life prediction compared to tiliroside and losartan, which obtained poor and medium remarks, respectively. This may indicate that maslinic acid may not require frequent dosing to attain the necessary exposure in the system and eventually exhibit its pharmacological effect. In addition, Reference [56] indicated that this scheme of pharmacokinetic analysis may still be improved when the

compound is modified so that its polar groups are increased to achieve a more hydrophilic structure.

Toxicity prediction of hit compounds and the standard drug was assessed through hERG inhibition, human hepatotoxicity (HHT), drug-induced liver injury (DILI) assessment, and AMES toxicity. These parameters were measured using two categories (positive and negative) with empirical decisions that serve as the probability that a particular category will occur. The following toxicity measures were selected because these were the common main concerns in drug development [64–66]. Furthermore, the early assessment and discoveries related to these toxicity parameters are essential to optimize the drug and become safer therapeutic agents [67].

Firstly, the potassium channels encoded by the human ether-á-go-go related genes (hERG) are crucial for cardiac action potential repolarization [68]. When blocked, hERG channels obstruct the flow of ions out of the cell, causing prolonged QT, a measure of delayed cardiac repolarization that can eventually lead to deadly arrhythmias [68]. Secondly, both HHT and DILI are fit to evaluate the effect of drugs in the liver since this organ is the center for drug and xenobiotic metabolism and where medication-mediated toxic effects have the largest impact [69]. Specifically, the toxic effects are commonly described as the biochemical stress a drug may cause to the hepatocyte's mitochondria [70]. Lastly, the AMES test assesses the carcinogenic potential of a drug [71]. A compound that can cause mutation and alter the His operon gene toward activation may allow the bacteria to form colonies even in the histidine-lacking medium [72]. Based on the toxicity profile predictions, all tested compounds have a low chance of blocking the hERG channel. However, in terms of predictions on liver impact, both tiliroside and losartan obtained medium to high positive results, which means there is a higher tendency to damage the liver. Lastly, only tiliroside got a positive result for the carcinogenicity prediction, indicating a high chance of causing mutation.

In silico ADMET analysis has proven to be an essential tool in predicting the properties of natural compounds. Previous studies have all highlighted the potential of in silico methods in this area [73–76]. These assessments can provide information about the pharmacology of compounds, thereby reducing the risk of late-stage attrition in drug development [73]. For instance, curcumin has shown promising anti-cancer properties, but its low bioavailability is a challenge [77]. Similarly, the natural compound epigallocatechin gallate from green tea has been found to have desirable absorption and anti-cancer properties, but potential hepatotoxicity risks have been highlighted [78]. While in silico models are not a replacement for in vivo or in vitro methods, they can guide medicinal chemistry towards more ideal property spaces, minimizing the need for compound synthesis [79].

3.4. Alanine scanning analysis

For the verification of the binding of amino acids in the protein, alanine scanning revealed that the mutants Q149A, F364A, and P484A exhibited changes in binding affinities of $\Delta\Delta G = 7.9$, 2.7, and 0.4 kcal/mol, respectively (see Table 4). Q149A had the most significant difference among the mutants, while P484A had the lowest, accounting for a 92% and 4.7% reduction in binding energy, respectively. This suggests that the absence of Gln149 from the URAT-1-maslinic acid complex would significantly reduce the stability of their interaction, which could be associated with maslinic acid's ability to competitively inhibit UA reabsorption by URAT-1. Furthermore, the results highlighted the significance of Gln149 and found a possible mutation that might significantly disrupt the URAT-1-maslinic acid interaction [80]. Moreover, since Gln149 is one of the residues involved in the protein-substrate interaction, mutation in Gln149 may interfere with URAT-1's interaction with UA. This observation regarding the probable mechanism of maslinic acid in inhibiting URAT-1 is consensus with the findings from the binding assay performed where the known URAT-1 inhibitors benzbromarone, lesinurad, probenecid, and sulfinpyrazone exhibited similarities with UA, in their interaction to URAT-1, as they were seen to interact with similar residues that sit in proximity with each other which are found around the same binding pocket [36].

3.5. Molecular dynamics simulation analysis

The URAT-1-maslinic acid complex was further analyzed regarding its stability using MDS, where

Table 4. Changes in binding affinities ($\Delta\Delta G$) of the substituted residues that interacted with maslinic acid.

	Wild-type Binding Affinity, ΔG (kcal/mol)	Binding Affinity, ΔG (kcal/mol)	Reduction in Binding Affinity, ΔΔG (kcal/mol)
1. Wild type	−8.6	−8.6	0
2. Q149A	−8.6	−0.7	7.9
3. F364A	−8.6	−5.9	2.7
4. P484A	−8.6	−8.2	0.4

ideal and close to natural conditions were observed in the full atomic aspect [81]. Initially, the complex was relaxed before the production step, which led to a significant decrease in the potential energy of the complex from −3,907,976 to −5,405,054 kJ/mol, which was then exposed to constant NVT and NPT conditions for 100 ns as a means of mimicking ideal conditions. Consequently, the full MDS was performed for 10,000 ps, where the root mean square deviation (RMSD) and root mean square fluctuation (RMSF) statistics were calculated from the trajectory. It is worth noting that the duration of simulations can vary significantly depending on the specific systems being studied [82]. The generation of stable lines in the production phase indicates that equilibrated dynamics are obtained [83]. Based on Fig. 6, the free protein dynamics exhibited deviations from the beginning of the simulation until 5000 ps, where the plot stabilized around ~1 nm. Likewise, the RMSD behavior of the protein with maslinic acid exhibited two separate slightly stable equilibrium portions, one of which is from the beginning of the simulation until 3000 ps with the plot being stable around ~0.5 nm and another one from 4000 ps to 8000 ps where the plot has stabled around ~0.75 nm. However, RMSD values throughout the simulation should fall under the range from ~0.2 to 0.3 nm, as the fluctuation in this range implies promising stability in the complex, which was not satisfied in the MDS [84]. Nonetheless, the URAT-1-maslinic acid complex exhibited relatively low RMSD values vis-à-vis the protein backbone with an average of 0.6081 nm ± 0.1448 compared to the RMSD values of the free protein with an average of 0.9199 nm ± 0.2185. Therefore, the RMSD plot of the URAT-1-maslinic acid complex has a relatively stable behavior compared to the free protein. The RMSD value gave way to evaluating the initial conformation of the protein compared with the succeeding changes that took place during the simulation for 10,000 ps [85]. Likewise, the RMSF plot was also considered for the individual fluctuations of each amino acid residue. However, the modifications performed in the homology modeling step indicate that some portions of the protein were omitted because of the template protein's limitations [86]. This omission has caused an adjustment in the numbering of the residues. Moreover, it can be observed in Fig. 7 that most of the residues exhibited remarkable RMSF values that are also low except for residues beyond 400. Nonetheless, the RMSF values exhibited a relatively low mean RMSF of 0.2243 nm ± 0.1983 compared to the free protein with an average RMSF of 0.2565 nm ± 0.2442, suggesting stable dynamics at the expense of the interaction of URAT-1 with maslinic acid.

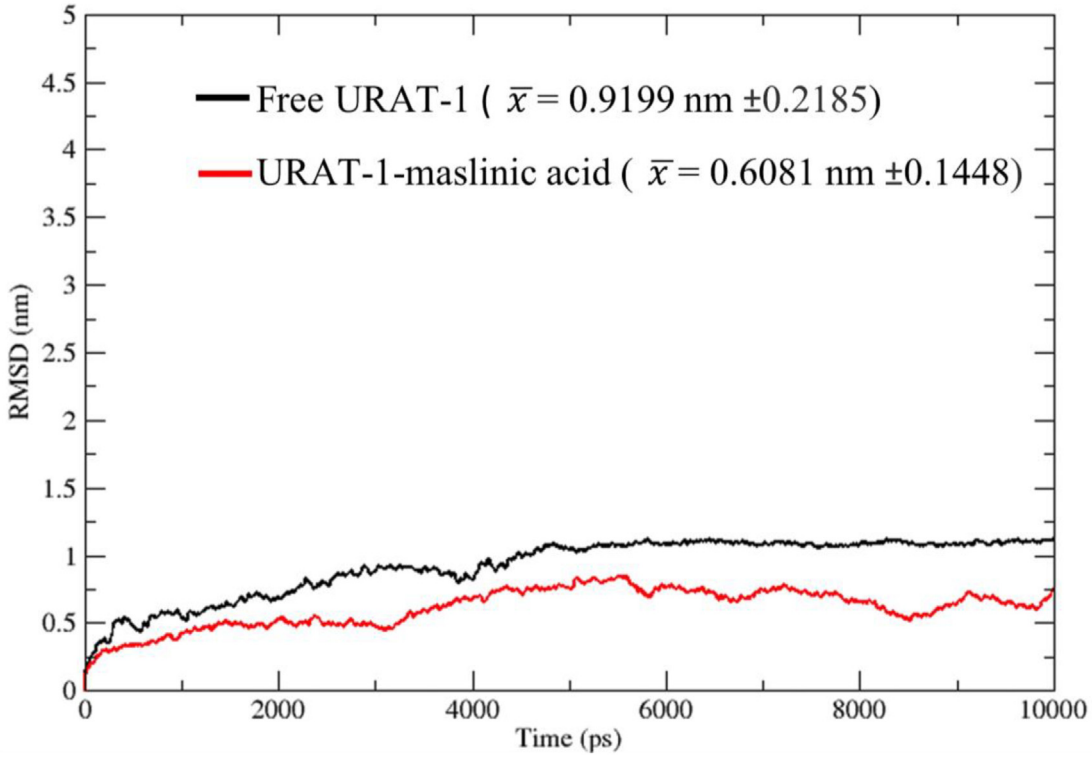

Fig. 6. Molecular dynamics analysis of the free URAT-1 vs. URAT-1-maslinic acid using root mean square deviation (RMSD).

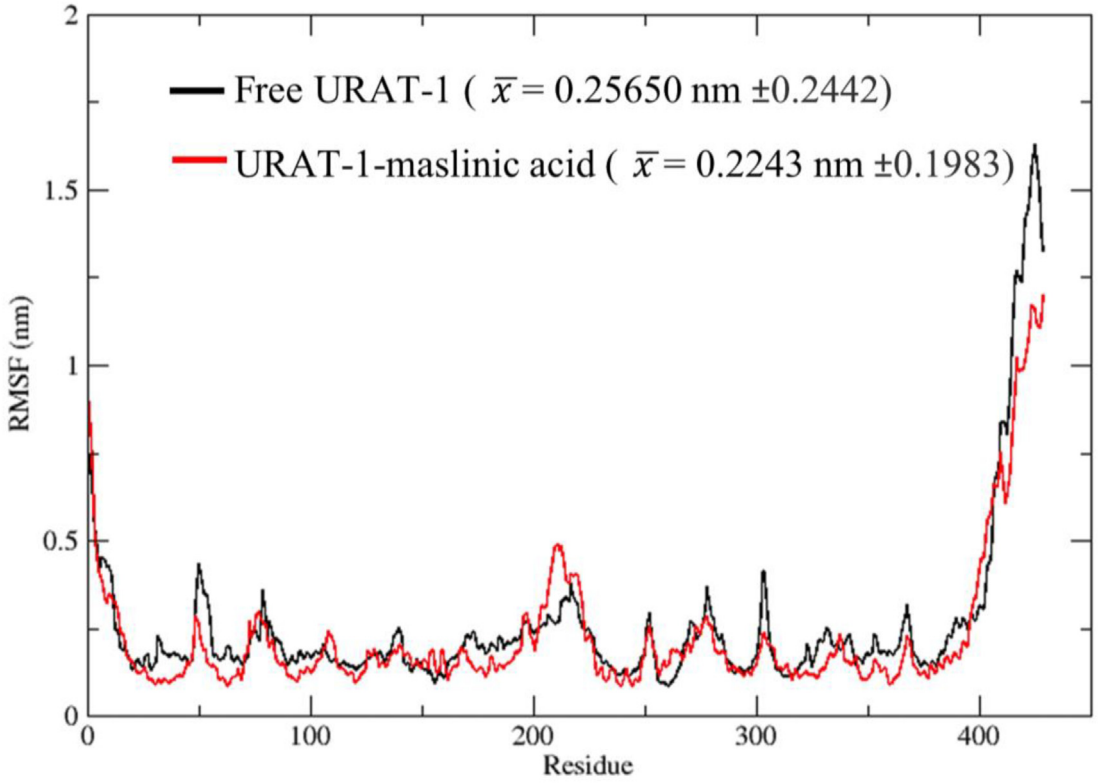

Fig. 7. Molecular dynamics analysis of the free URAT-1 vs. URAT-1-maslinic acid using root mean square fluctuation (RMSF) plot.

Furthermore, fluctuations of the residues may be perceived more specifically by considering the residues that have participated in the interaction between URAT-1 and maslinic acid. From the molecular docking analysis, maslinic acid interacted with Gln63, Phe240, and Pro360 (originally Gln149, Phe364, and Pro484, respectively). These residues exhibited RMSF values of 0.0860 nm, 0.0863 nm, 0.0915 nm, respectively. It can be observed that the RMSF values of the residues responsible for the interaction are much lower compared to the RMSF values of the mentioned residues in the free protein, which are 0.1959 nm, 0.1155 nm, 0.1858 nm, respectively. Similarly, the RMSF values and binding energy reduction (ΔΔG) in the alanine scanning of Gln63, Phe240, and Pro360 portray similarities in their trend. Thus, the replacement of Gln63 has substantially diminished the binding energy of the complex in alanine scanning, which has the lowest value of RMSF among the residues responsible for the interaction as calculated through MDS. This concept proposes that the interaction of the compound with the protein heavily relies on the stability of each amino acid residue's conformation [61].

Ultimately, the molecular dynamics simulation did not only expound on the stability of URAT-1-maslinic acid interactions. It also granted implications regarding the applications of structural stability towards the robustness of the interaction. Moreover, comparing the URAT-1-maslinic acid complex against the free URAT-1 in terms of their dynamics has revealed that maslinic acid may have contributed to the further stabilization of the protein structure. This notion also suggests that the interaction of maslinic acid to URAT-1 may have a high probability of ensuing due to the comparatively favorable dynamics of the protein in the presence of maslinic acid.

4. Conclusion

Inhibiting URAT-1 to lower serum uric acid (sUA) levels is another biochemical perspective of anti-hyperuricemic agents. It is significant to reduce the sUA concentrations because excessive amounts of uric acid in the body may lead to gout and related diseases. In the present study, homology modeling, molecular docking, pharmacological assessment, alanine scanning mutagenesis, and molecular dynamics simulation were successfully applied to confirm the potential inhibitory effects of compounds in *D. philippinensis*. It was found that among the compounds, maslinic acid and tiliroside can efficiently inhibit the transporter and were

identified as hit compounds. Further, maslinic acid was predicted to exhibit notable and promising pharmacological properties among such compounds. Therefore, this compound has a huge potential to progress to another research stage in drug discovery. This investigation revealed that the bioactive compounds found in *D. philippinensis* showed novel breakthroughs using emerging computational tools, which provided great results that may aid in developing antihyperuricemic treatments. It is worth noting that the present study may provide essential information for efficiently streamlining the drug discovery process, offering rapid, cost-effective, and ethically responsible methods for predicting the profiles of potential antihyperuricemic agents. This early-stage screening is crucial in identifying promising candidates and reducing the risk of late-stage failures.

While the present study can help predict and validate the biological activity of compounds like maslinic acid found in *D. philippinensis,* future research studies should conduct in vitro and in vivo analyses to determine the efficacy and safety of maslinic acid in a biological context. Long-term studies are essential to uncover any possible adverse effects and establish the clinical viability of the compound. Lastly, it is imperative to undertake extensive research to identify more novel compounds from *D. philippinensis.* This could further elucidate the plant's capacity to yield effective antihyperuricemic substances.

Funding

This research was conducted without any external funding or financial support.

Ethics information

Not applicable. This study is a purely in silico analysis with no animal or human subjects.

Acknowledgments

The authors would like to acknowledge the colleagues and professors from the Department of Biochemistry and the Faculty of Pharmacy at the University of Santo Tomas for their guidance and valuable insights during the composition of this study.

References

[1] H. Hassan, M.H. Alosami, H. Al-Hakeim, M. AL-Rufaie, Gout: a reviewing of the recent literature, East African, J Biophys Sci Chem 15 (2023) 51–58, https://doi.org/10.21608/eajbsc.2023.308858.

[2] J.E. Pizzorno, M.T. Murray, H. Joiner-Bey, Gout, the Clinician's Handbook of Natural Medicine, Elsevier. 2016, https://doi.org/10.1054/ctim.2002.0503.

[3] Y.T. Ding, J. Zhang, X.X. Zhou, P.C. Zhao, Analysis and distribution of purine components in common foods and condiments, Food Ferment Ind 46 (2020) 276–281, https://doi.org/10.13995/j.cnki.11-1802/ts.023617.

[4] Z. Zhao, Y. Jiang, L. Li, Y. Chen, Y. Li, Q. Lan, T. Wu, C. Lin, Y. Cao, K.S. Nandakumar, P. Zhou, Y. Tian, J. Pang, Structural insights into the atomistic mechanisms of uric acid recognition and translocation of human urate anion transporter 1, ACS Omega 5 (2020) 33421–33432, https://doi.org/10.1021/acsomega.0c05360.

[5] D.B. Mount, C.Y. Kwon, K. Zandi-Nejad, Renal urate transport, Rheum Dis Clin N Am 32 (2006) 313–vi, https://doi.org/10.1016/j.rdc.2006.02.006.

[6] A. Enomoto, H. Endou, Roles of organic anion transporters (OATs) and a urate transporter (URAT1) in the pathophysiology of human disease, Clin Exp Nephrol 9 (2005) 195–205, https://doi.org/10.1007/s10157-005-0368-5.

[7] O. Krystufkova, J. Vencovsky, S. Ruzickova, J. Sinkora, J. Niederlova, C.A. Power, C. Plater-Zyberk, Intracellular expression of CXCR3 on rheumatoid arthritis synovial tissue cells, Arthritis Res 3 (2001) 21, https://doi.org/10.1186/ar190.

[8] J.A. Singh, A. Gaffo, Gout epidemiology and comorbidities, Semin Arthritis Rheum 50 (2020) 11–16, https://doi.org/10.1016/j.semarthrit.2020.04.008.

[9] L.N. Helget, T.R. Mikuls, Health disparities in gout, Curr Opin Rheumatol 36 (2024) 120–125, https://doi.org/10.1097/BOR.0000000000000996.

[10] C.F. Kuo, M.J. Grainge, W. Zhang, M. Doherty, Global epidemiology of gout: prevalence, incidence and risk factors, Nat Rev Rheumatol 11 (2015) 649–662, https://doi.org/10.1038/nrrheum.2015.91.

[11] S.J. Chang, Y.C. Ko, T.N. Wang, F.T. Chang, F.F. Cinkotai, C.J. Chen, High prevalence of gout and related risk factors in Taiwan's Aborigines, J Rheumatol 24 (1997) 1364–1369.

[12] A. So, N. Busso, A magic bullet for gout? Ann Rheum Dis 68 (2009) 1517–1519, https://doi.org/10.1136/ard.2009.112508.

[13] S.E. Sattui, A.L. Gaffo, Treatment of hyperuricemia in gout: current therapeutic options, latest developments and clinical implications, Ther Adv Musculoskel Dis 8 (2016) 145–159, https://doi.org/10.1177/1759720X16646703.

[14] J.N. Miner, P.K. Tan, D. Hyndman, S. Liu, C. Iverson, P. Nanavati, D.T. Hagerty, K. Manhard, Z. Shen, J.L. Girardet, L.T. Yeh, R. Terkeltaub, B. Quart, Lesinurad, a novel oral compound for gout, acts to decrease serum uric acid through inhibition of urate transporters in the kidney, Arthritis Res Ther 18 (2016) 214, https://doi.org/10.1186/s13075-016-1107-x.

[15] P. Siripiyasing, K. Silawong, T. Thooptianrat, R. Sudmoon, N. Babayan, L. Khondkaryan, L. Apresyan, T. Tanee, A. Chaveerach, Screening of phytochemicals, toxicities, and activities of three Dillenia species, J Herbmed Pharmacol 11 (2022) 339–347, https://doi.org/10.34172/jhp.2022.39.

[16] R.A.S. Macahig, K. Matsunami, H. Otsuka, Chemical studies on an endemic Philippine plant: sulfated glucoside and seco-A-ring triterpenoids from *Dillenia philippinensis*, Chem Pharm Bull (Tokyo) 59 (2011) 397–401, https://doi.org/10.1248/cpb.59.397.

[17] M.R.N. Martillana, A. Lou, T. Artificio, G.R.A. Nolasco, A.N. Parco, P.C.M. Santos, Anti-hyperglycemic effects of *Dillenia philippinensis* Rolfe. (Dilleniaceae) Crude Leaf Extracts on Hyperglycemic Mice, Thesis, Far Eastern University. 2014.

[18] C.Y. Ragasa, A.B. Alimboyoguen, C.C. Shen, Antimicrobial triterpenes from *Dillenia philippinensis*, Philippine Sci 46 (2010) 78–87, https://doi.org/10.3860/psci.v46i0.1454.

[19] S.S. Ansari, P.H. Diño, A.L. Castillo, L.A. Santiago, Antioxidant activity, xanthine oxidase inhibition and acute oral toxicity of *Dillenia philippinensis* Rolfe (Dilleniaceae) leaf extract, J Pharm Pharmacogn Res 9 (2021) 846–858, https://doi.org/10.56499/jppres21.1106_9.6.846.

[20] S. Kumar, V. Kumar, O. Prakash, Enzymes inhibition and antidiabetic effect of isolated constituents from *Dillenia indica*, BioMed Res Int 2013 (2013) 382063, https://doi.org/10.1155/2013/382063.
[21] M.N. Parvin, M.S. Rahman, M.S. Islam, M.A. Rashid, Chemical and biological investigations of *Dillenia indica* Linn, Bangladesh J Pharmacol 4 (2009) 2, https://doi.org/10.3329/bjp.v4i2.2758.
[22] L. Saiful Yazan, N. Armania, Dillenia species: a review of the traditional uses, active constituents and pharmacological properties from pre-clinical studies, Pharmaceut Biol 52 (2014) 890–897, https://doi.org/10.3109/13880209.2013.872672.
[23] C.C. Lima, R.P.L. Lemos, L.M. Conserva, Dilleniaceae family: an overview of its ethnomedicinal uses, biological and phytochemical profile, J Pharmacogn Phytochem 3 (2014) 181–204.
[24] X. Li, C. Li, C. Cui, M. Li, M. Fan, Chemical constituents of *Dillenia kerrii* and their activities on antitumor and anti-hypoxia in vitro, Chin J Med Chem 19 (2009) 130–134.
[25] H. Harada, Y. Matsushita, M. Yodo, M. Nakamura, Y. Yonetani, Studies on uricosuric diuretics. I. 6,7-Dichloro-5-sulfamoyl-2,3-dihydrobenzofuran-2-carboxylic acids, Chem Pharmaceut Bull 35 (1987) 3195–3214, https://doi.org/10.1248/cpb.35.3195.
[26] M.D. Hanwell, D.E. Curtis, D.C. Lonie, T. Vandermeersch, E. Zurek, G.R. Hutchison, Avogadro: an advanced semantic chemical editor, visualization, and analysis platform, J Cheminf 4 (2012) 17, https://doi.org/10.1186/1758-2946-4-17.
[27] J.L. Perry, N. Dembla-Rajpal, L.A. Hall, J.B. Pritchard, A three-dimensional model of human organic anion transporter 1, J Biol Chem 281 (2006) 38071–38079, https://doi.org/10.1074/jbc.M608834200.
[28] B. Webb, A. Sali, Comparative protein structure modeling using MODELLER, Curr Protoc Bioinform 54 (2016) 5.6.1–5.6.37, https://doi.org/10.1002/cpbi.3.
[29] H. Land, M.S. Humble, YASARA: a tool to obtain structural guidance in biocatalytic investigations, Methods Mol Biol 1685 (2018) 43–67, https://doi.org/10.1007/978-1-4939-7366-8_4.
[30] R.A. Laskowski, M.W. MacArthur, D.S. Moss, J.M. Thornton, PROCHECK: a program to check the stereochemical quality of protein structures, J Appl Crystallogr 26 (1993) 283–291, https://doi.org/10.1107/S0021889892009944.
[31] A.M. Henzler, S. Urbaczek, B. Schulz, M. Rarey, A flexible-hydrogen interaction model for protein-ligand docking, J Cheminf 4 (2012) 14, https://doi.org/10.1186/1758-2946-4-S1-P14.
[32] W. Tian, C. Chen, X. Lei, J. Zhao, J. Liang, CASTp 3.0: computed atlas of surface topography of proteins, Nucleic Acids Res 46 (2018) 363–367, https://doi.org/10.1093/nar/gky473.
[33] O. Trott, A.J. Olson, AutoDock Vina: improving the speed and accuracy of docking with a new scoring function, efficient optimization, and multithreading, J Comput Chem 31 (2010) 455–461, https://doi.org/10.1002/jcc.21334.
[34] A. Daina, O. Michielin, V. Zoete, SwissADME: a free web tool to evaluate pharmacokinetics, drug-likeness and medicinal chemistry friendliness of small molecules, Sci Rep 7 (2017) 42717, https://doi.org/10.1038/srep42717.
[35] G. Xiong, Z. Wu, J. Yi, L. Fu, Z. Yang, C. Hsieh, M. Yin, X. Zeng, C. Wu, A. Lu, X. Chen, T. Hou, D. Cao, ADMETlab 2.0: an integrated online platform for accurate and comprehensive predictions of ADMET properties, Nucleic Acids Res 49 (2021) 5–14, https://doi.org/10.1093/nar/gkab255.
[36] P.K. Tan, T.M. Ostertag, J.N. Miner, Mechanism of high-affinity inhibition of the human urate transporter URAT1, Sci Rep 6 (2016) 1–13, https://doi.org/10.1038/srep34995.
[37] M.R. Barnes, I.C. Gray, Bioinformatics for Geneticists, John Wiley & Sons, Chichester, England. 2007, https://doi.org/10.1002/9780470059180.ch13.
[38] E. Hellsberg, G.F. Ecker, A. Stary-Weinzinger, L.R. Forest, A structural model of the human serotonin transporter in an outward-occluded state, PLoS One 14 (2019) 217377, https://doi.org/10.1371/journal.pone.0217377.
[39] S. Muthu, B. Durairaj, Molecular docking studies on interaction of *Annona muricata* compounds with antiapoptotic proteins Bcl-2 and survivin, Sky J Biochem Res 5 (2016) 14–17.
[40] D. Afriza, W.H. Suriyah, S.J.A. Ichwan, In silico analysis of molecular interactions between the anti-apoptotic protein survivin and dentatin, nordentatin, and quercetin, J Phys Conf 1073 (2018) 032001, https://doi.org/10.1088/1742-6596/1073/3/032001.
[41] I.O. Adedotun, M. Abdul-Hammed, B.A. Hamzat, A. Adepoju, M. Akinboade, T. Afolabi, U. Ismail, Molecular docking, ADMET analysis, and bioactivity studies of phytochemicals from *Phyllanthus niruri* as potential inhibitors of hepatitis C virus NSB5 polymerase, J Indian Chem Soc 99 (2022) 100321, https://doi.org/10.1016/j.jics.2021.100321.
[42] G.M. Morris, M. Lim-Wilby, Molecular docking, Methods Mol Biol 443 (2008) 365–382, https://doi.org/10.1007/978-1-59745-177-2_19.
[43] C.A. Lipinski, Drug-like properties and causes of poor solubility and poor permeability, J Pharmacol Toxicol Methods 44 (2000) 235–249, https://doi.org/10.1016/s1056-8719(00)00107-6.
[44] Z. Disdier, S. Savoye, R.V.H. Dagnelie, Effect of solutes structure and pH on the n-octanol/water partition coefficient of ionizable organic compounds, Chemosphere 304 (2022) 135155, https://doi.org/10.1016/j.chemosphere.2022.135155.
[45] F. Ditzinger, D.J. Price, A.R. Ilie, N.J. Köhl, S. Jankovic, G. Tsakiridou, S. Aleandri, L. Kalantzi, R. Holm, A. Nair, C. Saal, B. Griffin, M. Kuentz, Lipophilicity and hydrophobicity considerations in bio-enabling oral formulations approaches - a PEARRL review, J Pharm Pharmacol 71 (2019) 464–482, https://doi.org/10.1111/jphp.12984.
[46] K. Soliman, F. Grimm, C.A. Wurm, A. Egner, Predicting the membrane permeability of organic fluorescent probes by the deep neural network-based lipophilicity descriptor DeepFl-LogP, Sci Rep 11 (2021) 6991, https://doi.org/10.1038/s41598-021-86460-3.
[47] J. Caldwell, I. Gardner, N. Swales, An introduction to drug disposition: the basic principles of absorption, distribution, metabolism, and excretion, Toxicol Pathol 23 (1995) 102–114, https://doi.org/10.1177/019262339502300202.
[48] M.S. Alqahtani, M. Kazi, M.A. Alsenaidy, M.Z. Ahmad, Advances in oral drug delivery, Front Pharmacol 12 (2021) 618411, https://doi.org/10.3389/fphar.2021.618411.
[49] S. Rathod, H. Desai, R. Patil, J. Sarolia, Non-ionic surfactants as a p-glycoprotein (P-gp) efflux inhibitor for optimal drug delivery- a concise outlook, AAPS PharmSciTech 23 (2022) 55, https://doi.org/10.1208/s12249-022-02211-1.
[50] A.K. Green, S.L. Haley, M.D. Dearing, D.M. Barnes, W.H. Karasov, Intestinal capacity of p-glycoprotein is higher in the juniper specialist, *Neotoma stephensi*, than the sympatric generalist, *Neotoma albigula*, Comp Biochem Physiol Mol Integr Physiol 139 (2004) 325–333, https://doi.org/10.1016/j.cbpb.2004.09.017.
[51] Z.Y. Ibrahim, A. Uzairu, G.A. Shallangwa, S.E. Abechi, Pharmacokinetic predictions and docking studies of substituted aryl amine-based triazolopyrimidine designed inhibitors of *Plasmodium falciparum* dihydroorotate dehydrogenase (PfDHODH), Futur J Pharm Sci 7 (2021) 133, https://doi.org/10.1186/s43094-021-00288-2.
[52] H. Kadry, B. Noorani, L. Cucullo, A blood–brain barrier overview on structure, function, impairment, and biomarkers of integrity, Fluids Barriers CNS 17 (2020) 69, https://doi.org/10.1186/s12987-020-00230-3.
[53] P. Gardiner, R.J. Cox, K. Grime, Plasma protein binding as an optimizable parameter for acidic drugs, Drug Metabol Dispos 47 (2019) 865–873, https://doi.org/10.1124/dmd.119.087163.
[54] V. Mulpuru, N. Mishra, In silico prediction of fraction unbound in human plasma from chemical fingerprint using automated machine learning, ACS Omega 6 (2021) 6791–6797, https://doi.org/10.1021/acsomega.0c05846.

[55] J.A. Roberts, F. Pea, J. Lipman, The clinical relevance of plasma protein binding changes, Clin Pharmacokinet 52 (2013) 1–8, https://doi.org/10.1007/s40262-012-0018-5.
[56] B.J. Pleuvry, Modes of drug elimination, Anaesth Intensive Care Med 6 (2005) 277–279, https://doi.org/10.1383/anes.2005.6.8.277.
[57] M. Zhao, J. Ma, M. Li, Y. Zhang, B. Jiang, X. Zhao, C. Huai, L. Shen, N. Zhang, L. He, S. Qin, Cytochrome P450 enzymes and drug metabolism in humans, Int J Mol Sci 22 (2021) 12808, https://doi.org/10.3390/ijms222312808.
[58] B. Mittal, S. Tulsyan, S. Kumar, R.D. Mittal, G. Agarwal, Cytochrome P450 in cancer susceptibility and treatment, Adv Clin Chem 71 (2015) 77–139, https://doi.org/10.1016/BS.ACC.2015.06.003.
[59] Y. Wang, J. Xing, Y. Xu, N. Zhou, J. Peng, Z. Xiong, X. Liu, X. Luo, C. Luo, K. Chen, M. Zheng, H. Jiang, In silico ADME/T modeling for rational drug design, Q Rev Biophys 48 (2015) 488–515, https://doi.org/10.1017/s0033583515000190.
[60] D.B. Kell, R. Goodacre, Metabolomics and systems pharmacology: why and how to model the human metabolic network for drug discovery, Drug Discov Today 19 (2014) 171–182, https://doi.org/10.1016/j.drudis.2013.07.014.
[61] J. Kirchmair, M.J. Williamson, J.D. Tyzack, L. Tan, P.J. Bond, A. Bender, R.C. Glen, Computational prediction of metabolism: sites, products, SAR, P450 enzyme dynamics, and mechanisms, J Chem Inf Model 52 (2012) 617–648, https://doi.org/10.1021/ci200542m.
[62] A. Cua, K. Krock, R. Thomas, A. Pesce, Estimates of drug metabolism using drug excretion concentrations, ACLS (Ann Clin Lab Sci) 53 (2023) 460–468.
[63] O. Ekpenyong, X. Gao, J. Ma, C. Cooper, L. Nguyen, O.A. Olaleye, D. Liang, H. Xie, Pre-clinical pharmacokinetics, tissue distribution and physicochemical studies of CLBQ14, a novel methionine aminopeptidase inhibitor for the treatment of infectious diseases, Drug Des Dev Ther 14 (2020) 1263–1277, https://doi.org/10.2147/DDDT.S238148.
[64] A. Karim, M. Lee, T. Balle, A. Sattar, CardioTox net: a robust predictor for hERG channel blockade based on deep learning meta-feature ensembles, J Cheminf 13 (2021) 60, https://doi.org/10.1186/s13321-021-00541-z.
[65] D. Singh, W.C. Cho, G. Upadhyay, Drug-induced liver toxicity and prevention by herbal antioxidants: an overview, Front Physiol 6 (2015) 363, https://doi.org/10.3389/fphys.2015.00363.
[66] K.H. Hsu, B.H. Su, Y.S. Tu, O.A. Lin, Y.J. Tseng, Mutagenicity in a molecule: identification of core structural features of mutagenicity using a scaffold analysis, PLoS One 11 (2016) 148900, https://doi.org/10.1371/journal.pone.0148900.
[67] L.K. Vora, A.D. Gholap, K. Jetha, R.R.S. Thakur, H.K. Solanki, V.P. Chavda, Artificial intelligence in pharmaceutical technology and drug delivery design, Pharmaceutics 15 (2023) 1916, https://doi.org/10.3390/pharmaceutics15071916.
[68] S.M. Lamothe, J. Guo, W. Li, T. Yang, S. Zhang, The human ether-a-go-go-related gene (hERG) potassium channel represents an unusual target for protease-mediated damage, J Biol Chem 291 (2016) 20387–20401, https://doi.org/10.1074/jbc.M116.743138.
[69] F.A. Atienzar, E.A. Blomme, M. Chen, P. Hewitt, J.G. Kenna, G. Labbe, F. Moulin, F. Pognan, A.B. Roth, L. Suter-Dick, O. Ukairo, R.J. Weaver, Y. Will, D.M. Dambach, Key challenges and opportunities associated with the use of in vitro models to detect human DILI: integrated risk assessment and mitigation plans, BioMed Res Int 2016 (2016) 9737920, https://doi.org/10.1155/2016/9737920.
[70] L. Yuan, N. Kaplowitz, Mechanisms of drug-induced liver injury, Clin Liver Dis 17 (2013) 507–518, https://doi.org/10.1016/j.cld.2013.07.002.
[71] U. Vijay, S. Gupta, P. Mathur, P. Suravajhala, P. Bhatnagar, Microbial mutagenicity assay: ames test, Bio-Protocol 8 (2018) 2763, https://doi.org/10.21769/BioProtoc.2763.
[72] P. McCarren, C. Springer, L. Whitehead, An investigation into pharmaceutically relevant mutagenicity data and the influence on Ames predictive potential, J Cheminf 3 (2011) 51, https://doi.org/10.1186/1758-2946-3-51.
[73] F. Yamashita, M. Hashida, In silico approaches for predicting ADME properties of drugs, Drug Metabol Pharmacokinet 19 (2004) 327–338, https://doi.org/10.2133/dmpk.19.327.
[74] G. Yan, X. Wang, Z. Chen, X. Wu, J. Pan, Y. Huang, G. Wan, Z. Yang, In-silico ADME studies for new drug discovery: from chemical compounds to Chinese herbal medicines, Curr Drug Metabol 18 (2017) 535–539, https://doi.org/10.2174/1389200218666170316094104.
[75] K.K. Chohan, S.W. Paine, N.J. Waters, Advancements in predictive in silico models for ADME, Curr Chem Biol 2 (2008) 215–228, https://doi.org/10.2174/187231308785739747.
[76] D. Butina, M.D. Segall, K. Frankcombe, Predicting ADME properties in silico: methods and models, Drug Discov Today 7 (2002) 83–88, https://doi.org/10.1016/s1359-6446(02)02288-2.
[77] A.K. Panda, D. Chakraborty, I. Sarkar, T. Khan, G. Sa, New insights into therapeutic activity and anticancer properties of curcumin, J Exp Pharmacol 9 (2017) 31–45, https://doi.org/10.2147/JEP.S70568.
[78] S.R. Lin, C.H. Chang, C.F. Hsu, M.J. Tsai, H. Cheng, M.K. Leong, P.J. Sung, J.C. Chen, C.F. Weng, Natural compounds as potential adjuvants to cancer therapy: preclinical evidence, Br J Pharmacol 177 (2020) 1409–1423, https://doi.org/10.1111/bph.14816.
[79] M.P. Gleeson, A. Hersey, S. Hannongbua, In-silico ADME models: a general assessment of their utility in drug discovery applications, Curr Top Med Chem 11 (2011) 358–381, https://doi.org/10.2174/156802611794480927.
[80] C. Kristensen, T. Kjeldsen, F.C. Wiberg, L. Schäffer, M. Hach, S. Havelund, J. Bass, D.F. Steiner, A.S. Andersen, Alanine scanning mutagenesis of insulin, J Biol Chem 272 (1997) 12978–12983, https://doi.org/10.1074/jbc.272.20.12978.
[81] T.A. Collier, T.J. Piggot, J.R. Allison, Molecular dynamics simulation of proteins, Methods Mol Biol 2073 (2020) 311–327, https://doi.org/10.1007/978-1-4939-9869-2_17.
[82] R.C. Bernardi, M.C.R. Melo, K. Schulten, Enhanced sampling techniques in molecular dynamics simulations of biological systems, Biochim Biophys Acta 1850 (2015) 872–877, https://doi.org/10.1016/j.bbagen.2014.10.019.
[83] A. Smith, X. Dong, V. Raghavan, An overview of molecular dynamics simulation for food products and processes, Processes 10 (2022) 119, https://doi.org/10.3390/pr10010119.
[84] F. Lameh, A.Q. Baseer, A.G. Ashiru, Comparative molecular docking and molecular-dynamic simulation of wild-type and mutant carboxylesterase with BTA-hydrolase for enhanced binding to plastic, Eng Life Sci 22 (2021) 13–29, https://doi.org/10.1002/elsc.202100083.
[85] K. Sargsyan, C. Grauffel, C. Lim, How molecular size impacts RMSD applications in molecular dynamics simulations, J Chem Theor Comput 13 (2017) 1518–1524, https://doi.org/10.1021/acs.jctc.7b00028.
[86] T.M. Allison, E. Reading, I. Liko, A.J. Baldwin, A. Laganowsky, C.V. Robinson, Quantifying the stabilizing effects of protein-ligand interactions in the gas phase, Nat Commun 6 (2015) 8551, https://doi.org/10.1038/ncomms9551.